NAS 1.14:D-8528

AUG 19 197

NASA TECHNICAL NOTE

NASA TN D-8528

COMPLETED
ORIGINAL

NASA TN D-8528

ELASTOHYDRODYNAMIC LUBRICATION OF ELLIPTICAL CONTACTS FOR MATERIALS OF LOW ELASTIC MODULUS

I - Fully Flooded Conjunction

Bernard J. Hamrock and Duncan Dowson

Lewis Research Center
Cleveland, Ohio 44135

NATIONAL AERONAUTICS AND SPACE ADMINISTRATION • WASHINGTON D. C. • AUGUST 1977

30

1 Report No	2 Government Accession No	3 Recipient's Catalog No
NASA TN D-8528		

4 Title and Subtitle	5 Report Date
ELASTOHYDRODYNAMIC LUBRICATION OF ELLIPTICAL CONTACTS FOR MATERIALS OF LOW ELASTIC MODULUS I - FULLY FLOODED CONJUNCTION	August 1977
	6 Performing Organization Code

7 Author(s)	8 Performing Organization Report No
Bernard J. Hamrock, Lewis Research Center; and Duncan Dowson, Leeds University, Leeds, England	E-9216
	10 Work Unit No

9 Performing Organization Name and Address	11 Contract or Grant No
National Aeronautics and Space Administration Lewis Research Center Cleveland, Ohio 44135	
	13 Type of Report and Period Covered
12 Sponsoring Agency Name and Address	Technical Note
National Aeronautics and Space Administration Washington, D.C. 20546	14 Sponsoring Agency Code

15 Supplementary Notes

16 Abstract

Our earlier studies of elastohydrodynamic lubrication of conjunctions of elliptical form are applied to the particular and interesting situation exhibited by materials of low elastic modulus. By modifying the procedures we outlined in an earlier publication, the influence of the ellipticity parameter k and the dimensionless speed U, load W, and material G parameters on minimum film thickness for these materials has been investigated. The ellipticity parameter was varied from 1 (a ball-on-plate configuration) to 12 (a configuration approaching a line contact). The dimensionless speed and load parameters were varied by 1 order of magnitude. Seventeen different cases were used to generate the following minimum- and central-film-thickness relations: $\bar{H}_{min} = 7.43(1 - 0.85\, e^{-0.31k})U^{0.65}W^{-0.21}$; and $\bar{H}_c = 7.32(1 - 0.72\, e^{-0.28k})U^{0.64}W^{-0.22}$. Contour plots are presented that illustrate in detail the pressure distribution and film thickness in the conjunction.

17 Key Words (Suggested by Author(s))	18 Distribution Statement
Elastohydrodynamic lubrication; Materials of low elastic modulus; Seals; Human joints; Elastomeric-material machine elements	Unclassified - unlimited STAR Category 37

19 Security Classif (of this report)	20 Security Classif (of this page)	21 No of Pages	22 Price*
Unclassified	Unclassified	29	A03

* For sale by the National Technical Information Service, Springfield, Virginia 22161

ELASTOHYDRODYNAMIC LUBRICATION OF ELLIPTICAL CONTACTS FOR MATERIALS OF LOW ELASTIC MODULUS

I - FULLY FLOODED CONJUNCTION

by Bernard J. Hamrock and Duncan Dowson*

Lewis Research Center

SUMMARY

Our earlier studies of elastohydrodynamic lubrication of conjunctions of elliptical form are applied to the particular and interesting situation exhibited by materials of low elastic modulus. By modifying the procedures we outlined in an earlier publication, the influence of the ellipticity parameter k and the dimensionless speed U, load W, and material G parameters on minimum film thickness for these materials has been investigated. The ellipticity parameter was varied from 1 (a ball-on-plate configuration) to 12 (a configuration approaching a line contact). The dimensionless speed and load parameters were varied by 1 order of magnitude. Seventeen different cases were used to generate the following minimum- and central-film-thickness relations:

$$\tilde{H}_{min} = 7.43(1 - 0.85\, e^{-0.31k})U^{0.65}W^{-0.21}$$

$$\tilde{H}_{c} = 7.32(1 - 0.72\, e^{-0.28k})U^{0.64}W^{-0.22}$$

Contour plots are presented that illustrate in detail the pressure distribution and film thickness in the conjunction.

---

* Professor of Mechanical Engineering, Leeds University, Leeds, England.

INTRODUCTION

Only in recent years has the complete numerical solution of the isothermal elastohydrodynamic lubrication (EHL) of elliptical contacts successfully emerged. The analysis requires the simultaneous solution of the elasticity and Reynolds equations. The authors' approach to the theoretical solution has been presented in two previous publications (refs. 1 and 2). The first of these publications (ref. 1) presents an elasticity model in which the conjunction is divided into equal rectangular regions with a uniform pressure applied over each region. The second (ref. 2) gives a complete approach to the solution of the elastohydrodynamic lubrication problem for point contacts.

The most important practical aspect of the EHL point-contact theory (ref. 2) is the determination of the minimum film thickness within the contact. That is, the prediction of a film of adequate thickness is extremely important for the successful operation of machine elements in which these thin, continuous, fluid films occur. In a recent paper by the authors (ref. 3) the fully flooded results obtained from the theory given in references 1 and 2 were presented. A fully flooded condition is said to exist when the inlet distance of the conjunction ceases to influence in any significant way the minimum film thickness. In reference 3 the influence of the ellipticity parameter and the dimensionless speed, load, and material parameters on minimum film thickness was investigated. Thirty-four different cases were used in obtaining the fully flooded minimum-film-thickness formula.

In reference 4 the basic theory developed in references 1 and 2 was used to study the effect of lubricant starvation on the pressure and film thickness within the conjunction. A simple expression for the dimensionless inlet boundary distance was obtained. This inlet boundary distance defines whether a fully flooded or a starved condition exists in the contact. Fifteen cases, in addition to three presented in reference 3, were used to obtain simple expressions for the minimum and central film thicknesses in a starved conjunction.

The work presented in references 1 to 4 related to a material of high elastic modulus (e.g., steel). The work presented in the present report is for a material of <u>low</u> elastic modulus (e.g., nitrile rubber). For such materials the distortions are large even with light loads. Another feature of the EHL of low-elastic-modulus materials is the negligible effect of pressure on the viscosity of the lubricating fluid. Engineering applications in which elastohydrodynamic lubrication is important for low-elastic-modulus materials include seals, human joints, tires, and elastomeric-material machine elements.

The problem of line contacts, where side leakage of the fluid is ignored, has been solved theoretically for low-elastic-modulus materials by Herrebrugh (ref. 5), Dowson and Swales (ref. 6), and Baglin and Archard (ref. 7). The solutions of references 5

and 6 were obtained numerically and are based on simultaneous solutions of the hydrodynamic and elasticity equations; the analytical solution of reference 7 relied on the assumption of a simplified form for the film shape in the contact region. Biswas and Snidle (ref. 8) used the approach of reference 7 to solve the point-contact (ball on plate) situation. The present work represents, to the best of the authors' knowledge, the first attempt at a complete numerical solution of the problem of isothermal elastohydrodynamic lubrication of elliptical contacts for low-elastic-modulus materials. In this report, no assumptions are made as to the pressure or film thickness within the contact, and compressibility and viscous effects are considered.

SYMBOLS

a	semimajor axis of contact ellipse
b	semiminor axis of contact ellipse
D_1	$\left(\frac{\tilde{H}_{min} - H_{min}}{H_{min}}\right) 100$
D_2	$\left(\frac{\tilde{H}_c - H_c}{H_c}\right) 100$
E	modulus of elasticity
E'	$\frac{2}{\left(\frac{1-\nu_A^2}{E_A} + \frac{1-\nu_B^2}{E_B}\right)}$
F	normal applied load
G	dimensionless material parameter, $E'/p_{iv,as}$
H	dimensionless film thickness, h/R_x
H_c	dimensionless central film thickness obtained from EHL elliptical contact theory
$\tilde{H}_c$	dimensionless central film thickness obtained from least-squares fit of data
H_{min}	dimensionless minimum film thickness obtained from EHL elliptical contact theory
$\overline{H}_{min}$	dimensionless film thickness - speed parameter, $H_{min}U^{-0.5}$

$\left\{\bar{H}_{min}\right\}_B$ dimensionless film thickness - speed parameter from ref. 8

$\left\{\bar{H}_{min}\right\}_H$ dimensionless film thickness - speed parameter from present analysis

$\left\{\bar{H}_{min}\right\}_J$ dimensionless film thickness - speed parameter from unpublished data by W. E. Jamison of Clemson University

$\left\{\bar{H}_{min}\right\}_K$ dimensionless film thickness - speed parameter from ref. 9

$\hat{H}_{min}$ dimensionless minimum film thickness obtained from EHL elliptical contact theory for materials of high elastic modulus (ref. 3)

$\tilde{H}_{min}$ dimensionless minimum film thickness obtained from least-squares fit of data

$H_{min, L}$ dimensionless minimum film thickness for line contact

H_o constant, initially estimated

h film thickness

k ellipticity parameter, a/b

M_P dimensionless load-speed parameter, $WU^{-0.75}$

P dimensionless pressure, p/E'

P_D dimensionless pressure difference

P_{Hz} dimensionless Hertzian pressure

p pressure

$p_{iv, as}$ asymptotic isoviscous pressure

R effective radius

r radius of curvature

S natural separation of elliptical solids

U dimensionless speed parameter, $u\eta_0/E'R_x$

u mean surface velocity in x-direction, $\frac{1}{2}(u_A + u_B)$

W dimensionless load parameter, $F/E'R_x^2$

w_{Hz} elastic deformation due to Hertzian pressure distribution

$w|_{P_D}$ elastic deformation due to pressure difference, from eq. (2)

$\left.\begin{matrix} x, X, \overline{X} \\ y, Y, \overline{Y} \end{matrix}\right\}$ coordinate systems defined in report

α pressure-viscosity coefficient

$\overline{\eta}$ dimensionless viscosity

η_0 atmospheric viscosity

ν Poisson's ratio

ρ lubricant density

$\overline{\rho}$ dimensionless density, ρ/ρ_0

ρ_0 atmospheric density

Subscripts:

A solid A

B solid B

x, y coordinate system defined in report

THEORETICAL FORMULATION

The basic theory developed in reference 2 is used here with some minor modifications. It was discovered that numerical convergence was considerably better if the dimensionless pressure was written as

$$P = P_{Hz} + P_D \tag{1}$$

P_{Hz} dimensionless Hertzian pressure

P_D dimensionless pressure difference

By making use of equation (1), the relevant Reynolds equation can be written as

$$\frac{\partial}{\partial X}\left(\frac{\overline{\rho}H^3}{\overline{\eta}}\frac{\partial P_D}{\partial X}\right) + \frac{1}{k^2}\frac{\partial}{\partial Y}\left(\frac{\overline{\rho}H^3}{\overline{\eta}}\frac{\partial P_D}{\partial Y}\right) + \frac{\partial}{\partial X}\left(\frac{\overline{\rho}H^3}{\overline{\eta}}\frac{\partial P_{Hz}}{\partial X}\right)$$

$$+\frac{1}{k^2}\frac{\partial}{\partial Y}\left(\frac{\overline{\rho}H^3}{\overline{\eta}}\frac{\partial P_{Hz}}{\partial Y}\right) = 12U\left(\frac{b}{R_x}\right)\frac{\partial(\overline{\rho}H)}{\partial X} \tag{2}$$

where $k = a/b$ is the ellipticity parameter. Since the Hertzian pressure is known, the solution of the Reynolds equation involves solving for P_D. In equation (2), compressibility and viscous effects are considered even though it was mentioned in the INTRODUCTION that the effect of pressure on viscosity and density is negligible.

The equation for the dimensionless film thickness is written as

$$H = H_o + \frac{\left(S + w_{Hz} + w|_{P_D}\right)}{R_x} \tag{3}$$

H_o constant (initially guessed)

S natural separation of elliptical solids

w_{Hz} elastic deformation due to Hertzian pressure distributions

$w|_{P_D}$ elastic deformation due to pressure difference obtained from eq. (2)

The evaluation of the elastic deformation is exactly that used in references 1 and 2.

The nodal structure used for obtaining all the results is shown in figure 1. It should be noted from this figure that, because of the dimensionless representation of the coordinates, the actual Hertzian contact ellipse becomes a circle regardless of the value of k. The nodal structure shown in figure 1 was arrived at after much exploration in which the number of nodes in the semimajor and semiminor axes, as well as the distance from the center of the contact to the edges of the computing zone, was varied.

DIMENSIONLESS GROUPING

The same dimensionless grouping of parameters used in the analysis of elastohydrodynamic lubrication of high-elastic-modulus materials (ref. 3) is used herein:

Dimensionless film thickness:

$$H = \frac{h}{R_x} \tag{4}$$

Ellipticity parameter:

$$k = \frac{a}{b} \tag{5}$$

Dimensionless speed parameter:

$$U = \frac{\eta_0 u}{E' R_x} \tag{6}$$

Dimensionless load parameter:

$$W = \frac{F}{E' R_x^2} \tag{7}$$

Dimensionless material parameter:

$$G = \frac{E'}{p_{iv,\,as}} \tag{8}$$

where $p_{iv,\,as}$ is the asymptotic isoviscous pressure obtained from Roelands (ref. 10). The asymptotic isoviscous pressure can be approximated by the inverse of the pressure-viscosity coefficient, $p_{iv,\,as} \approx (1/\alpha)$.

The dimensionless film thickness can be written as

$$H = f(k, U, W, G) \tag{9}$$

The most important practical aspect of the elastohydrodynamic lubrication elliptical contact theory is the determination of the minimum film thickness within the conjunction. Therefore, in the fully flooded results presented herein, the dimensionless parameters k, U, W, and G were varied, and the effect upon minimum film thickness studied. Care was taken to ensure that all results were in the elastic region.

EFFECT OF ELLIPTICITY OF ELASTIC CONJUNCTION

The ellipticity parameter is a function of the radii of curvature of the solids only (r_{Ax}, r_{Bx}, r_{Ay}, and r_{By}). The radii of curvature in the x-direction for both solids A and B are used in defining the dimensionless speed and load parameters. Therefore, only the radius of curvature of solid B in the y-direction was changed in varying k from 1 (a ball-on-plate configuration) to 12 (a configuration approaching a line contact). In doing this, the dimensionless speed, load, and material parameters were held constant at

$$\left.\begin{aligned} U &= 0.1028\times10^{-7} \\ W &= 0.4405\times10^{-3} \\ G &= 0.4276 \end{aligned}\right\} \tag{10}$$

Table I gives seven values of the ellipticity parameter and the corresponding minimum film thickness as obtained from the EHL elliptical contact theory. Having these seven pairs of data, the object was to determine an equation that would describe how the ellipticity parameter affects the minimum film thickness. The general form of this equation can be written as

$$\left(1 - \frac{H_{min}}{H_{min,\,L}}\right) = Ae^{Bk} \tag{11}$$

A least-squares exponential curve fit to the seven pairs of data points

$$k_i, \left[\left(1 - \frac{H_{min}}{H_{min,\,L}}\right)_i\right] \qquad i = 1, \ldots, 7$$

was used in obtaining values for A and B in equation (11). Besides a least-squares fit, a coefficient of determination r^2 was obtained. The value of r^2 reflects the fit of the data to the resulting equation: 1 being a perfect fit, and zero the worst possible fit. The minimum film thickness for a line contact $H_{min,\,L}$ used in equation (11) was determined by finding the $H_{min,\,L}$ that gives a coefficient of determination closest to 1. This value of $H_{min,\,L}$ turned out to be 240.0×10^{-6}, with a corresponding coefficient of determination of 0.9908, which is an excellent fit. Furthermore, the values of A and B in equation (11), as obtained from the least-squares fit, are

$$A = 0.8488 \approx 0.85 \tag{12}$$

$$B = -0.3115 \approx -0.31 \tag{13}$$

From equations (11) to (13), the following equation can be written, which shows the effec effect of k on $\bar{H}_{min}$:

$$\tilde{H}_{min} \propto (1 - 0.85\, e^{-0.31k}) \tag{14}$$

Figure 2 shows the variation of the ratio $H_{min}/H_{min,L}$ with k for the EHL high-elastic-modulus analysis (ref. 3) and the EHL low-elastic-modulus analysis (present results). If we assume that the minimum film thickness obtained from the EHL elliptical analysis can only be obtained to an accuracy of 3 percent, we find a limiting solution for line contact being approached for a k of 5 for the EHL high-elastic-modulus analysis and for a k of 11 for the EHL low-elastic-modulus analysis.

INFLUENCE OF SPEED

Changing only the surface velocity in the x-direction u causes the dimensionless speed parameter U to change while the other dimensionless parameters (k, W, and G) remain constant. The values at which these dimensionless parameters were held constant in the calculations were

$$\left.\begin{aligned} W &= 0.4405\times10^{-3} \\ k &= 6 \\ G &= 0.4276 \end{aligned}\right\} \tag{15}$$

Table I also gives the dimensionless speed parameter and the corresponding dimensionless minimum film thickness as obtained from the EHL elliptical contact theory. There are five different values of the dimensionless speed parameter covering 1 order of magnitude. Having these five pairs of data, the objective was to determine an equation that would describe how the speed affects the minimum film thickness. The general form of this equation can be written as

$$H_{min} = IU^{J} \tag{16}$$

By applying a least-squares power fit to the five pairs of data, $(U_i, H_{min,i})$, where $i = 1, \ldots, 5$, the values of I and J were found to be

$$I = 32.48 \tag{17}$$

$$J = 0.6505 \approx 0.65 \tag{18}$$

The coefficient of determination r^2 for these results was excellent at 0.9997. From equations (16) and (18) the effect of dimensionless speed on dimensionless minimum film thickness can be written as

$$\bar{H}_{min} \propto U^{0.65} \tag{19}$$

Figure 3 gives contour plots of dimensionless pressure for two extreme values of U, 0.05139×10^{-7} and 0.5139×10^{-7}. In these and all contour plots to be presented, the + symbol indicates the center of the Hertzian contact. Because of the dimensionless representation of the X and Y coordinates, the actual Hertzian contact ellipse becomes a circle regardless of the value of k. The Hertzian contact circle is shown in each figure by asterisks. At the top of each figure the contour labels and the corresponding values of dimensionless pressure are given. The inlet region is to the left, and the exit region to the right.

The pressure contours shown in figure 3 are nearly circular, or Hertzian. In figure 3(b), the high-speed case, the inlet pressure was higher than in the low-speed case shown in figure 3(a). Inside the contact the contour values of the dimensionless pressure were higher for the low-speed case (fig. 3(a)). The pressure spikes found when dealing with materials of high elastic modulus (ref. 3) were not in evidence in these solutions for low-elastic-modulus materials. The lack of a pressure spike is due to the lack of viscous effects of the fluid in the contact for low-elastic-modulus materials. This in turn is due to the fact that considerably less pressure is generated in a contact with low-elastic-modulus materials than in a contact with high-elastic-modulus materials.

Figure 4 shows contour plots of dimensionless film thickness for two values of U, 0.05139×10^{-7} and 0.5139×10^{-7}. Figure 4(a) shows two regions of minimum film thickness, close to the Hertzian circle and off to the side. Figure 4(b) shows one region of minimum film thickness, between the center of the contact and the Hertzian circle.

Figure 5 shows the variation of pressure and film thickness on the X-axis near the midplane of the conjunction for the same two values of U. For all the solutions for various speeds, the values of the dimensionless load, material, and ellipticity parameters were held fixed as described in equation (15). In figure 5 the pressure in the inlet region is higher for the higher speed ($U = 0.5139\times10^{-7}$) profile. It should be noted that these slight changes in pressure that occur wher the speed is increased by 1 order of magnitude result in a significant change in film thickness, as indicated by equation (19).

This illustrates most clearly the dominant effect of the dimensionless speed parameter on the minimum film thickness in elastohydrodynamic contacts for low-elastic-modulus materials. Similar results were found for high-elastic-modulus materials (ref. 3).

INFLUENCE OF LOAD

Changing only the normal applied load F in equation (7) causes the dimensionless load parameter W to change while the other dimensionless parameters (k, U, and G) remain constant. The values at which these parameters were held constant were

$$\left.\begin{aligned} U &= 0.1028\times10^{-7} \\ k &= 6 \\ G &= 0.4276 \end{aligned}\right\} \tag{20}$$

The load results presented in table I give the dimensionless load parameter and the corresponding minimum film thickness as obtained from the EHL elliptical contact theory. There are six different values of dimensionless load parameter covering 1 order of magnitude. Having these six pairs of data, the objective was to determine an equation that would describe how the dimensionless load affects the minimum film thickness. The general form of this equation can be written as

$$C = KW^{L} \tag{21}$$

where

$$C = \frac{H_{min}}{(1 - 0.85\, e^{-0.31k})U^{0.65}} \tag{22}$$

In equation (22) the exponents are rounded off to two significant figures so that any error could be absorbed in K, given in equation (21). By applying a least-squares power fit to the six pairs of data $[(W_i, C_i),\ i = 1, \ldots, 6]$, the values of K and L were found to be

$$K = 6.507 \tag{23}$$

$$L = -0.2075 \approx -0.21 \tag{24}$$

The coefficient of determination r^2 for these results was 0.9985, which is excellent. From equations (21), (22), and (24), the effect of load on minimum film thickness can be written as

$$\tilde{H}_{min} \propto W^{-0.21} \tag{25}$$

Figure 6 gives contour plots of dimensionless pressure for the two extreme values of W that were investigated, 0.2202×10^{-3} and 2.202×10^{-3}. Again the pressure contours were nearly circular, or Hertzian. The contour values were considerably higher for the high-load case (fig. 6(b)).

Contour plots of dimensionless film thickness for the same two values of W are shown in figure 7. In figure 7(a), for the low-load case ($W = 0.2202 \times 10^{-3}$), the minimum film thickness occurred directly behind the center of the contact; in figure 7(b), for the high-load case ($W = 2.202 \times 10^{-3}$), the minimum film thickness also occurred directly behind the center of the contact but closer to the Hertzian circle. The two C contours in figure 7(b) indicate a slight increase in film thickness before the minimum-film-thickness region is reached.

The variation of pressure and film thickness in the X-direction along a line close to the midplane of the conjunction is shown in figure 8 for two values of W. The values of U, G, and k were held fixed as described by equation (20) for all computations at various loads. In this figure, for a 1-order-of-magnitude change in the dimensionless load parameter, there is a considerable change in the pressure profile but not such a significant change in the film thickness profile.

MINIMUM-FILM-THICKNESS FORMULA

The proportionality expressions (14), (19), and (25) established how the minimum film thickness varied with the ellipticity, speed, and load parameters, respectively. This enabled a composite minimum-film-thickness formula for a fully flooded, isothermal, elastohydrodynamic elliptical contact for low-elastic modulus materials to be written as

$$\tilde{H}_{min} = 7.43(1 - 0.85\, e^{-0.31k})U^{0.65}W^{-0.21} \tag{26}$$

In equation (26) the constant 7.43 is different from that given in equation (23) to account for rounding off the load-parameter exponent.

Table I gives the values for the minimum film thickness obtained from the least-squares fit as defined by equation (26). The percentage difference between the minimum film thickness obtained from the EHL elliptical contact theory H_{min} and the minimum film thickness obtained from the least-squares fit equation $\tilde{H}_{min}$ is expressed as

$$D_1 = \left(\frac{\tilde{H}_{min} - H_{min}}{H_{min}} \right) 100 \tag{27}$$

In table I the values of D_1 are within the range -8 and +3.

It is sometimes more convenient to express the side-leakage factor in equation (26) in terms of the curvature ratio R_y/R_x instead of the ellipticity parameter through the following relation:

$$k = 1.03 \left(\frac{R_y}{R_x} \right)^{0.64} \tag{28}$$

where

$$\frac{1}{R_y} = \frac{1}{r_{Ay}} + \frac{1}{r_{By}} \tag{29}$$

$$\frac{1}{R_x} = \frac{1}{r_{Ax}} + \frac{1}{r_{Bx}} \tag{30}$$

Using equation (28) avoids the need to evaluate elliptic integrals of the first and second kinds in the determination of k. The minimum film thickness can thus be derived directly from a knowledge of the curvature of the contacting bodies (r_{Ax}, r_{Bx}, r_{Ay}, and r_{By}).

It is interesting to compare the equation for materials of <u>low</u> elastic modulus (eq. (26)) with the corresponding equation generated in reference 3 for materials of <u>high</u> elastic modulus

$$\hat{H}_{min} = 3.63\, U^{0.68} G^{0.49} W^{-0.073} (1 - e^{-0.68k}) \tag{31}$$

The powers of U in equations (26) and (31) are quite similar, but the power of W is much more significant for low-elastic-modulus materials. The expression showing the effect of the ellipticity parameter is of exponential form in both equations, but with quite different constants.

A major difference in equations (26) and (31) is the absence of a material parameter in the expression for the minimum film thickness for low-elastic-modulus materials. There are two reasons for this. One is the negligible effect of pressure on the viscosity of the lubricating fluid for low-elastic-modulus materials. The other is the way in which the role of elasticity is simply and automatically incorporated in the prediction of conjunction behavior through an increase in the size of the Hertzian contact zone corresponding to changes in load. As a check on the validity of this, case 9 of table I was repeated with the material changed from nitrile rubber to silicone rubber. This is recorded as case 17 (table I). As can be seen from equations (6) to (8), when the material (as expressed by E') is changed, not only does the material parameter change, but so do the dimensionless speed and load parameters. Only the ellipticity parameter can be held fixed. From table I, case 17, we find that the minimum film thickness from the EHL elliptical contact theory was 181.8×10^{-6}. The minimum film thickness from the least-squares fit (eq. (26)) turned out to be 182.5×10^{-6}. This clearly indicates a lack of dependence of the minimum film thickness for low-elastic-modulus materials on the material parameter.

CENTRAL-FILM-THICKNESS FORMULA

There is interest in knowing the central film thickness, in addition to the minimum film thickness, in elastohydrodynamic contacts. The procedure used in obtaining the central film thickness was the same as that used in obtaining the minimum film thickness and is not repeated here. The central-film-thickness formula for low-elastic-modulus materials obtained from the results is

$$\tilde{H}_c = 7.32(1 - 0.72\, e^{-0.28k})U^{0.64}W^{-0.22} \qquad (32)$$

Comparison of the central-film-thickness formula (eq. (32)) with the minimum-film-thickness formula (eq. (26)) reveals only slight differences.

Table II gives the 16 different cases used to obtain equation (32), as well as case 17, which is a check on equation (32). In this table, H_c corresponds to the central film thickness obtained from the EHL elliptical contact theory and $\tilde{H}_c$ corresponds to the central film thickness obtained from equation (32). The percentage difference between these two values is given by D_2 and is written as

$$D_2 = \left(\frac{\tilde{H}_c - H_c}{H_c} \right) 100 \tag{33}$$

In table II the values of D_2 are within the range -11 to +23.

The ratio of minimum to central film thickness evident in the computed values ranged from 70 to 83 percent, the average being 77 percent.

Comparison of Different Investigators' Results

To evaluate the dimensionless minimum-film-thickness equation (eq. (26)) developed in this report, a comparison was made between it, the numerical solution obtained by Biswas and Snidle (ref. 8), and the recent experimental findings of Jamison (unpublished data). Both are applicable only for $k = 1$.

From reference 8 the dimensionless minimum film thickness can be written as

$$\left\{ \bar{H}_{min} \right\}_B = 1.96 \, M_P^{-0.11} \tag{34}$$

where

$$\bar{H}_{min} = H_{min} \, U^{-0.5} \tag{35}$$

$$M_P = W U^{-0.75} \tag{36}$$

The dimensionless groups given in equations (35) and (36) were first used by Moes and Bosma (ref. 11).

The central-film-thickness equation obtained from the experimental results of Jamison can be written as

$$\left\{ \bar{H}_c \right\}_J = 2.4 \, M_P^{-0.075} \tag{37}$$

where

$$\bar{H}_c = H_c \, U^{-0.5} \tag{38}$$

Modifying equation (37) to provide a minimum-film-thickness equation by using the assumption that $\left\{\overline{H}_{min}\right\}_J = 0.78 \left\{H_c\right\}_J$ yields

$$\left\{\overline{H}_{min}\right\}_J = 1.87\, M_P^{-0.075} \tag{39}$$

Equations (34) and (39) are valid only for $k = 1$.

By making use of equations (35), (36), and table I equation (26) can be written as

$$\left\{\overline{H}_{min}\right\}_H = 8.53(1 - 0.85\, e^{-0.31k})M_P^{-0.21} \tag{40}$$

Therefore, for $k = 1$, equation (40) reduces to

$$\left\{\overline{H}_{min}\Big|_{k=1}\right\}_H = 3.21\, M_P^{-0.21} \tag{41}$$

Note the larger negative exponent in equation (41) than in either equations (34) or (39).

Figure 9 compares the different investigators' results from equations (34), (39), and (41). The three equations seem to agree quite well with each other. The present report's results are equivalent to the Biswas and Snidle theoretical results (ref. 8) at $M_P = 100$ and the Jamison experimental results at $M_P = 45$. Therefore, even though the exponent on M_P for the present results is larger than those obtained in reference 8 and by Jamison, the agreement is quite good for $k = 1$. Also shown in figure 9 is the rigid isoviscous solution obtained from Kapitza (ref. 9).

Figure 10 uses equation (40) to show the effect of the dimensionless parameter M_P on the dimensionless minimum film thickness for six values of the ellipticity parameter. As k increases, less change occurs in the dimensionless minimum film thickness. From this figure the dimensionless minimum film thickness can easily be obtained for known values of k and M_P.

Similarly, the equation for the dimensionless central film thickness can be written as

$$\left\{\overline{H}_c\right\}_H = 11.61(1 - 0.72\, e^{-0.28k})M_P^{-0.22} \tag{42}$$

Figure 11 uses equation (42) to show the effect of the dimensionless parameter M_P on the dimensionless central film thickness for six values of k.

CONCLUDING REMARKS

By modifying the procedures outlined by the authors in an earlier publication, the influence of the ellipticity parameter k and the dimensionless speed U, load W, and material G parameters on minimum film thickness for low-elastic-modulus materials has been investigated. The ellipticity parameter was varied from 1 (a ball-on-plate configuration) to 12 (a configuration approaching a line contact). The dimensionless speed and load parameters were varied by 1 order of magnitude. Seventeen different cases were used to generate the minimum- and central-film-thickness relations:

$$\tilde{H}_{min} = 7.43(1 - 0.85\, e^{-0.31k})U^{0.65}W^{-0.21}$$

$$\tilde{H}_c = 7.32(1 - 0.72\, e^{-0.28k})U^{0.64}W^{-0.22}$$

Contour plots have been presented that show in detail the pressure distribution and the film thickness in the conjunction.

The present report presents for the first time a complete theoretical film-thickness solution for the problem of isothermal elastohydrodynamic elliptical contacts for low-elastic-modulus materials operating under fully flooded conditions.

National Aeronautics and Space Administration,
Lewis Research Center,
Cleveland, Ohio, May 24, 1977,
505-04.

REFERENCES

1. Hamrock, Bernard J.; and Dowson, Duncan: Numerical Evaluation of the Surface Deformation of Elastic Solids Subjected to a Hertzian Contact Stress. NASA TN D-7774, 1974.

2. Hamrock, Bernard J.; and Dowson, Duncan: Isothermal Elastohydrodynamic Lubrication of Point Contacts. Part I - Theoretical Formulation. J. Lubr. Technol., vol. 98, no. 2, Apr. 1976, pp. 223-229.

3. Hamrock, Bernard J.; and Dowson, Duncan: Isothermal Elastohydrodynamic Lubrication of Point Contacts. Part III - Fully Flooded Results. J. Lubr. Technol., vol. 99, no. 2, Apr. 1977, pp. 264-276.

4. Hamrock, B. J.; and Dowson, D.: Isothermal Elastohydrodynamic Lubrication of Point Contacts. Part IV - Starvation Results. J. Lubr. Technol., vol. 99, no. 1, Jan. 1977, pp. 15-23.

5. Herrebrugh, K.: Solving the Incompressible and Isothermal Problem in Elastohydrodynamic Lubrication Through an Integral Equation. J. Lubr. Technol., vol. 90, no. 1, Jan. 1968, pp. 262-270.

6. Dowson, D.; and Swales, P. D.: The Development of Elastohydrodynamic Conditions in a Reciprocating Seal. Proceedings of the Fourth International Conference on Fluid Sealing, vol. 2, Paper 1, British Hydromechanics Research Association, 1969, pp. 1-9.

7. Baglin, K. P.; and Archard, J. F.: An Analytic Solution of the Elastohydrodynamic Lubrication of Materials of Low Elastic Modulus. Symposium on Elastohydrodynamic Lubrication, Inst. Mech. Engrs., p. 13.

8. Biswas, S.; and Snidle, R. W.: Elastohydrodynamic Lubrication of Spherical Surfaces of Low Elastic Modulus. J. Lubr. Technol., vol. 98, no. 4, Oct. 1976, pp. 524-529.

9. Kapitza, P. L.: Hydrodynamic Theory of Lubrication During Rolling. Zh. Tekh. Fiz., vol. 25, no. 2, 1955, p. 747.

10. Roelands, C. J. A.: Correlational Aspects of the Viscosity-Temperature-Pressure Relationship of Lubricating Oils. Druk V. R. B., Groningen, Netherlands, 1966.

11. Moes, H.; and Bosma, R.: Film Thickness and Traction in EHL at Point Contact. Symposium on Elastohydrodynamic Lubrication, Inst. Mech. Engrs., 1972, p. 149.

TABLE I. - DATA SHOWING EFFECT OF ELLIPTICITY, LOAD, SPEED, AND MATERIAL PARAMETERS ON MINIMUM FILM THICKNESS

Case	Ellipticity parameter, k	Dimensionless load parameter, W	Dimensionless speed parameter, U	Dimensionless material parameter, G	Minimum film thickness		Difference between H_{min} and $\tilde{H}_{min}$, D_1, percent	Results
					Obtained from EHL elliptical contact theory, H_{min}	Obtained from least-squares fit, $\tilde{H}_{min}$		
1	1	0.4405×10^{-3}	0.1028×10^{-7}	0.4276	88.51×10^{-6}	91.08×10^{-6}	+2.90	
2	2	↓	↓	↓	142.5	131.2	-7.93	
3	3				170.4	160.8	-5.63	
4	4				186.7	182.4	-2.30	Ellipticity
5	6				206.2	209.8	+1.75	
6	8				219.7	224.6	+2.23	
7	12				235.2	236.0	+.34	
8	6		.05139		131.8	133.7	+1.44	
9	↓		.1542		268.1	273.1	+1.86	Speed plus case 5
10			.2570		381.6	380.7	-.24	
11			.5139		584.7	597.3	+2.15	
12		.2202	.1028		241.8	242.7	+.37	
13		.6607	↓		190.7	192.7	+1.05	
14		1.101			170.5	173.1	+1.52	Load plus case 5
15		1.542			160.4	161.3	+.56	
16		2.202			149.8	149.7	-.07	
17		.1762	.06169	1.069	181.8	182.5	+.39	Material

TABLE II. - DATA SHOWING EFFECT OF ELLIPTICITY, LOAD, SPEED, AND MATERIAL PARAMETERS ON CENTRAL FILM THICKNESS

Case	Ellipticity parameter, k	Dimensionless load parameter, W	Dimensionless speed parameter, U	Dimensionless material parameter, G	Minimum film thickness		Difference between H_c and $\tilde{H}_c$ D_2, percent	Results
					Obtained from EHL elliptical contact theory, H_c	Obtained from least squares fit, $\tilde{H}_c$		
1	1	0.4405×10^{-3}	0.1028×10^{-7}	0.4276	114.9×10^{-6}	141.0×10^{6}	+22.72	} Ellipticity
2	2	↓	↓	↓	204.2	182.2	-10.77	
3	3				217.2	213.2	-1.84	
4	4				253.1	236.7	-6.48	
5	6				265.0	267.9	+1.09	
6	8				288.8	285.7	-1.07	
7	12		↓		307.1	301.7	-1.76	
8	6		.05139		171.7	171.9	+.12	} Speed plus case 5
9	↓		.1542		354.0	347.3	-1.89	
10			.2570		498.7	481.5	-3.45	
11		↓	.5139		743.7	750.3	+.89	
12		.2202	.1028		316.3	312.0	-1.36	} Load plus case 5
13		.6607	↓		235.1	245.0	+4.21	
14		1.101			221.5	219.0	-1.13	
15		1.542			192.6	203.4	+5.61	
16		2.202	↓	↓	196.6	188.0	-4.37	
17	↓	.1762	.06169	1.069	237.4	236.3	.46	Material

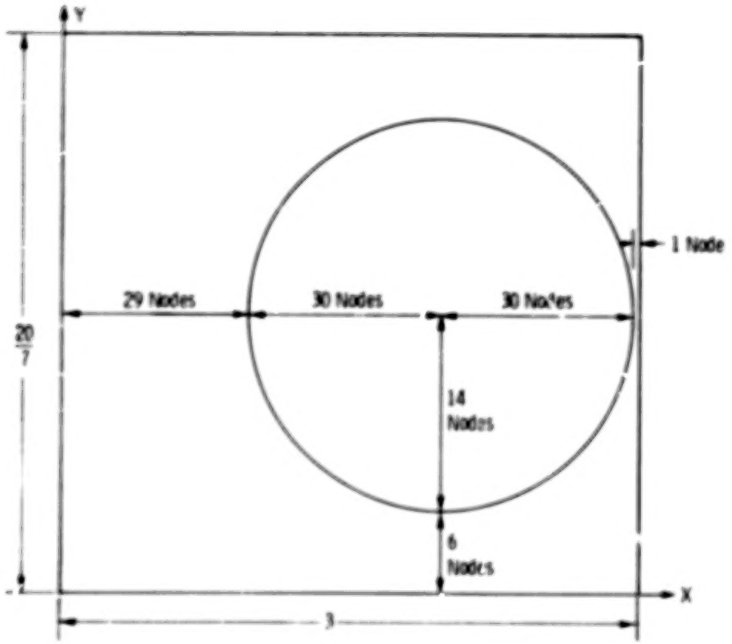

Figure 1. - Nodal structure used for numerical calculations.

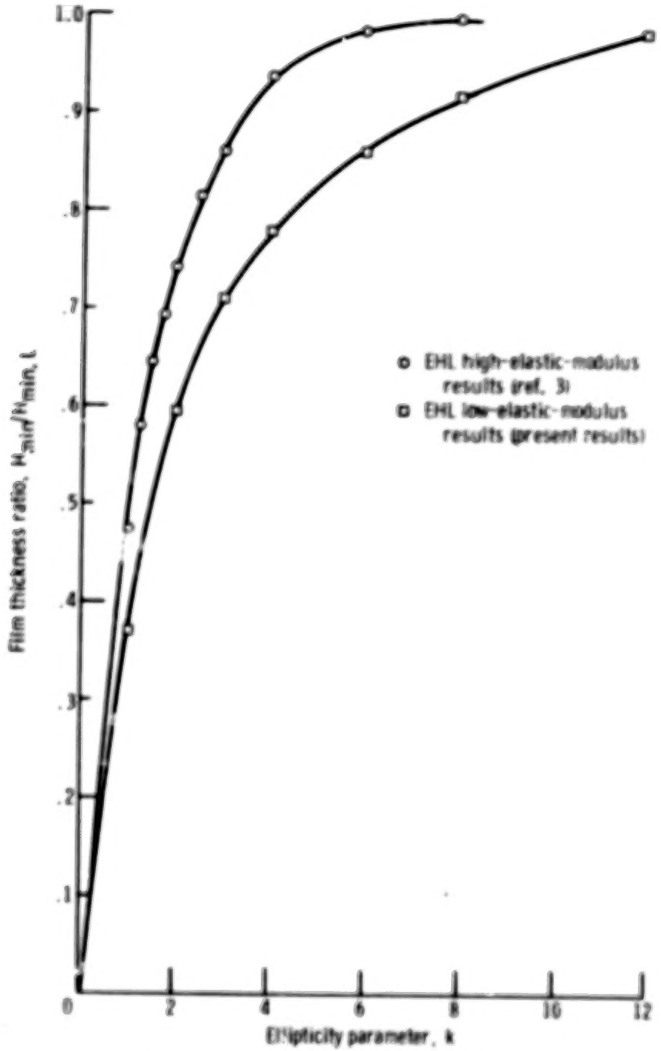

Figure 2. - Variation of ratio of dimensionless minimum film thickness to dimensionless minimum film thickness for a line contact with ellipticity parameter, for EHL high- and low-elastic-modulus analyses.

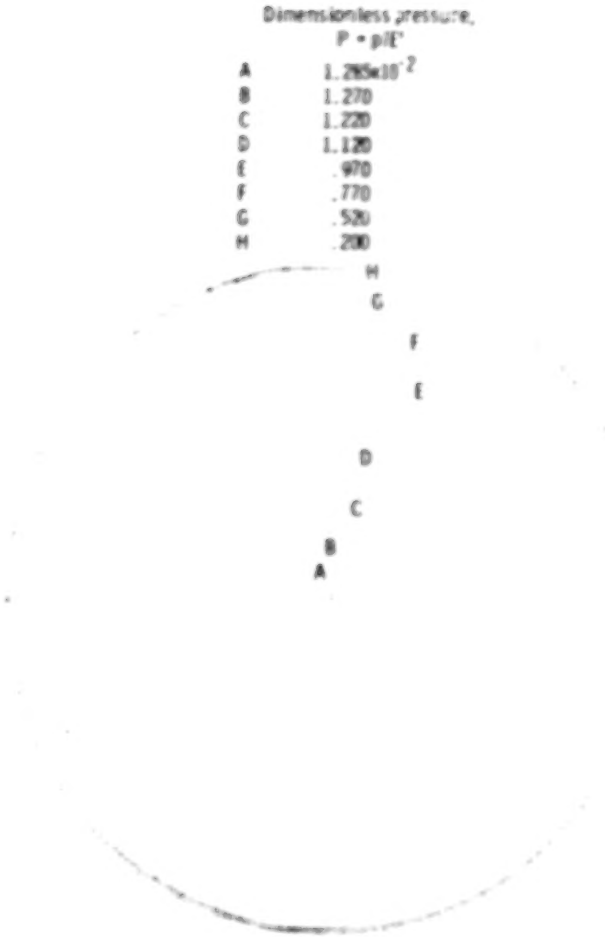

(a) Contour plot of dimensionless pressure for dimensionless speed U of 0.05139x10^{-7}.

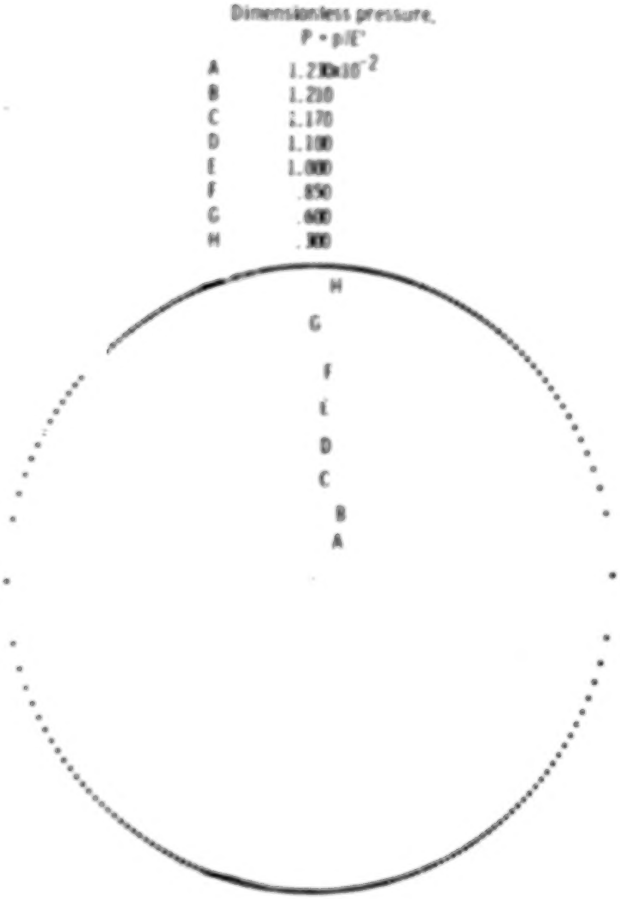

(b) Contour plot of dimensionless pressure for dimensionless speed U of 0.5139x10^{-7}.

Figure 3. - Contour plots of dimensionless pressure for dimensionless speed parameters U of 0.05139x10^{-7} and 0.5139x10^{-7}. The dimensionless parameters k, W, and G are held constant as defined in equation (15).

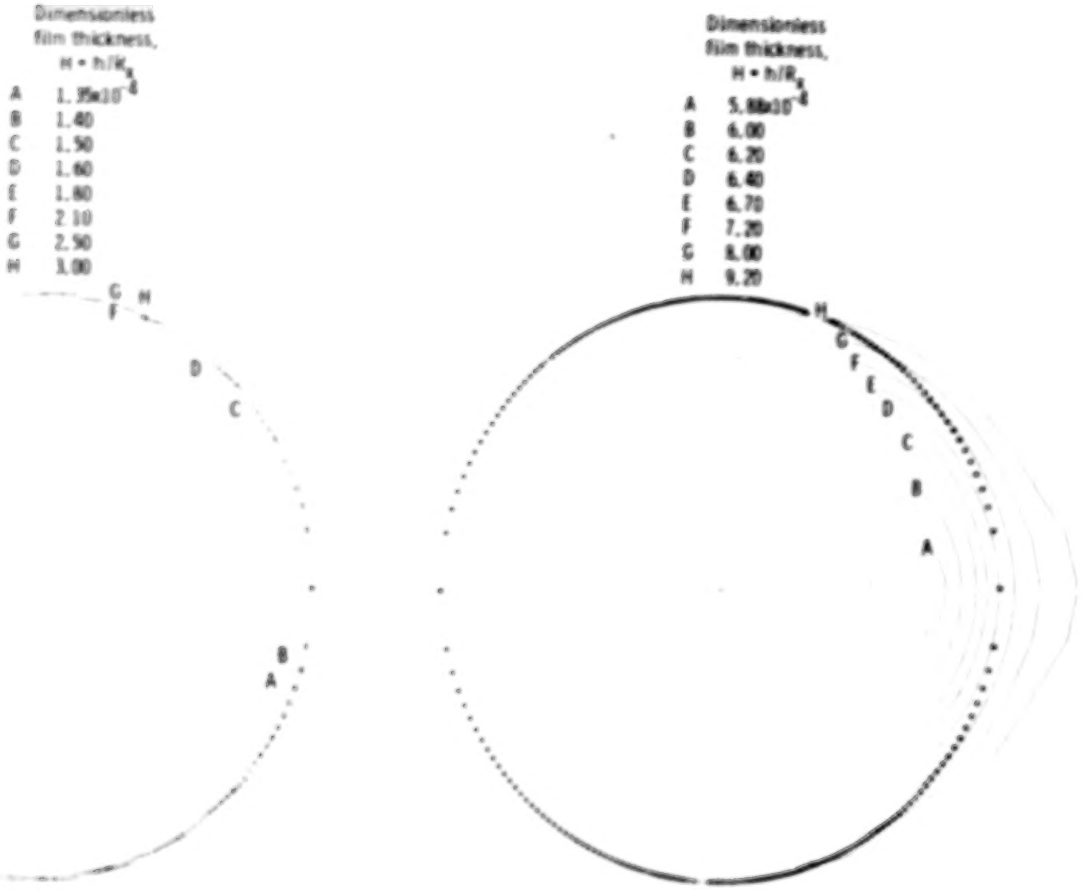

(a) Contour plot of dimensionless film thickness for dimensionless speed U of 0.05139×10^{-7}.

(b) Contour plot of dimensionless film thickness for dimensionless speed U of 0.5139×10^{-7}.

Figure 4. - Contour plots of dimensionless film thickness for dimensionless speed parameters U of 0.05139×10^{-7} and 0.5139×10^{-7}. The dimensionless parameters W and G are held constant as defined in equation (15).

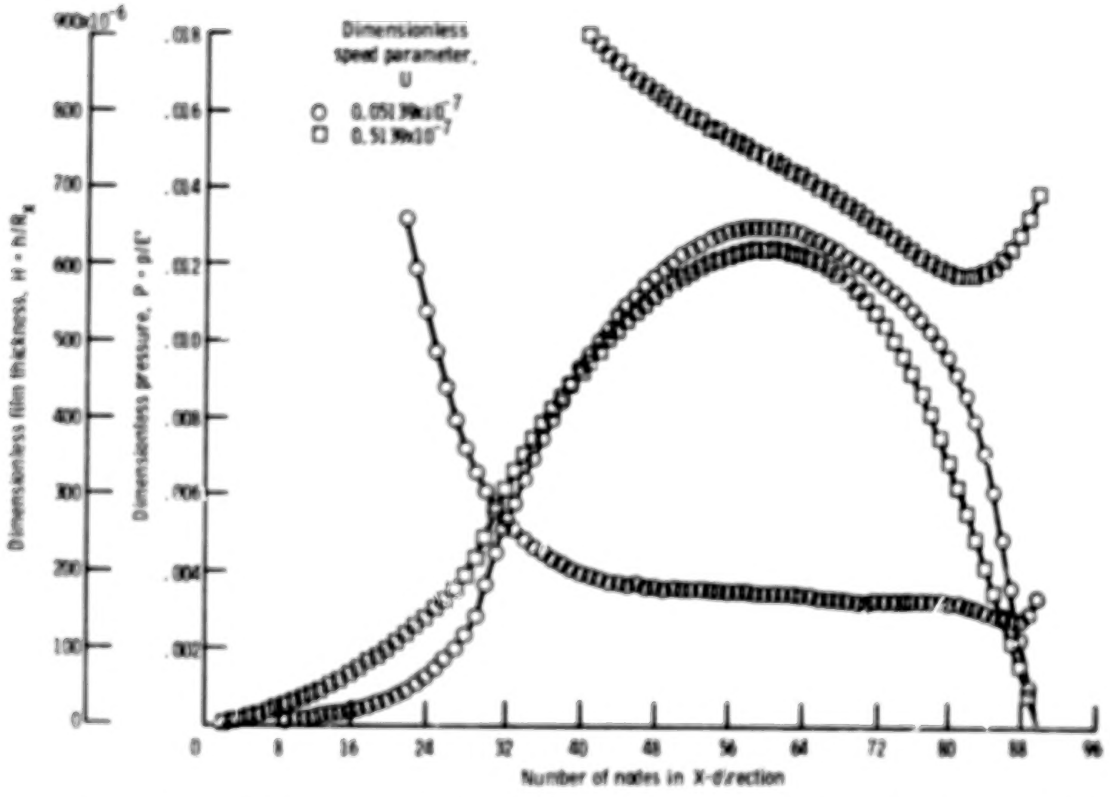
Dimensionless speed parameter, U
Dimensionless film thickness, H = h/R_x
Dimensionless pressure, P = p/Γ
Number of nodes in X-direction

Figure 5. - Variation of dimensionless pressure and film thickness on X-axis for dimensionless speed parameters U of 0.0513×10^{-7} and 0.513×10^{-7}. The value of Y is held fixed near axial center of contact.

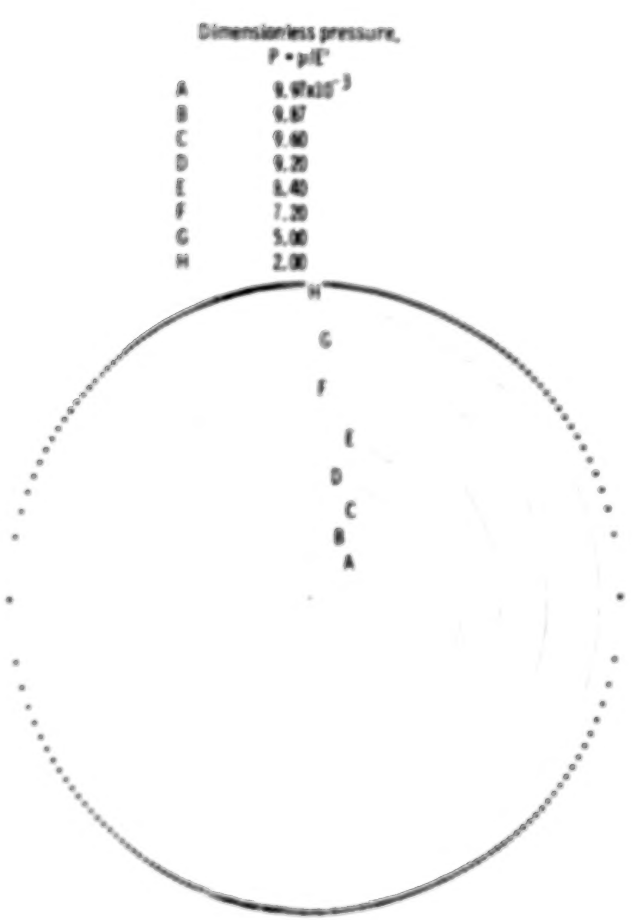

(a) Contour plot of dimensionless pressure for dimensionless load W of 0.2202×10^{-3}.

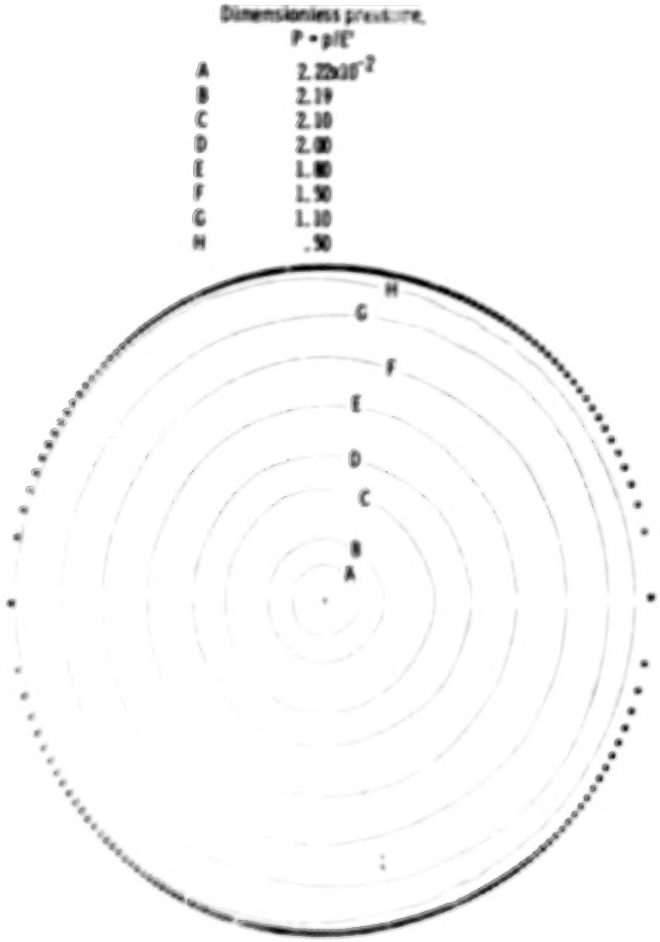

(b) Contour plot of dimensionless pressure for dimensionless load W of 2.202×10^{-3}.

Figure 6. - Contour plots of dimensionless pressure for dimensionless loads W of 0.2202×10^{-3} and 2.202×10^{-3}. The dimensionless parameters k, U, and G are held constant as defined in equation (20).

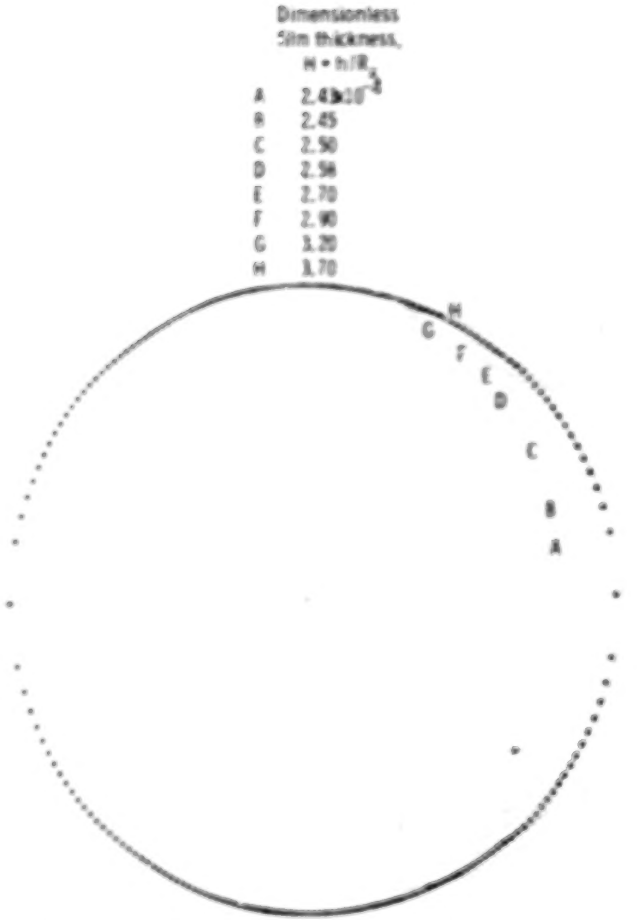

(a) Contour plot of dimensionless film thickness for dimensionless load W of 0.2202x10^-3.

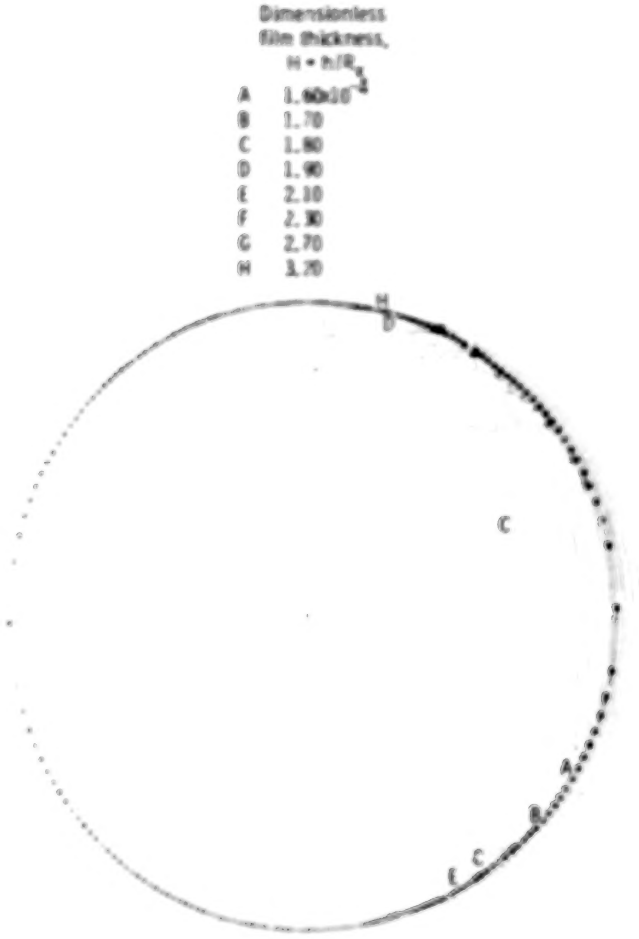

(b) Contour plot of dimensionless film thickness for dimensionless load W of 2.202x10^-3.

Figure 7. - Contour plots of dimensionless film thickness for dimensionless loads W of 0.2202x10^-3 and 2.202x10^-3. The dimensionless parameters k, U, and G are held constant as defined in equation (23).

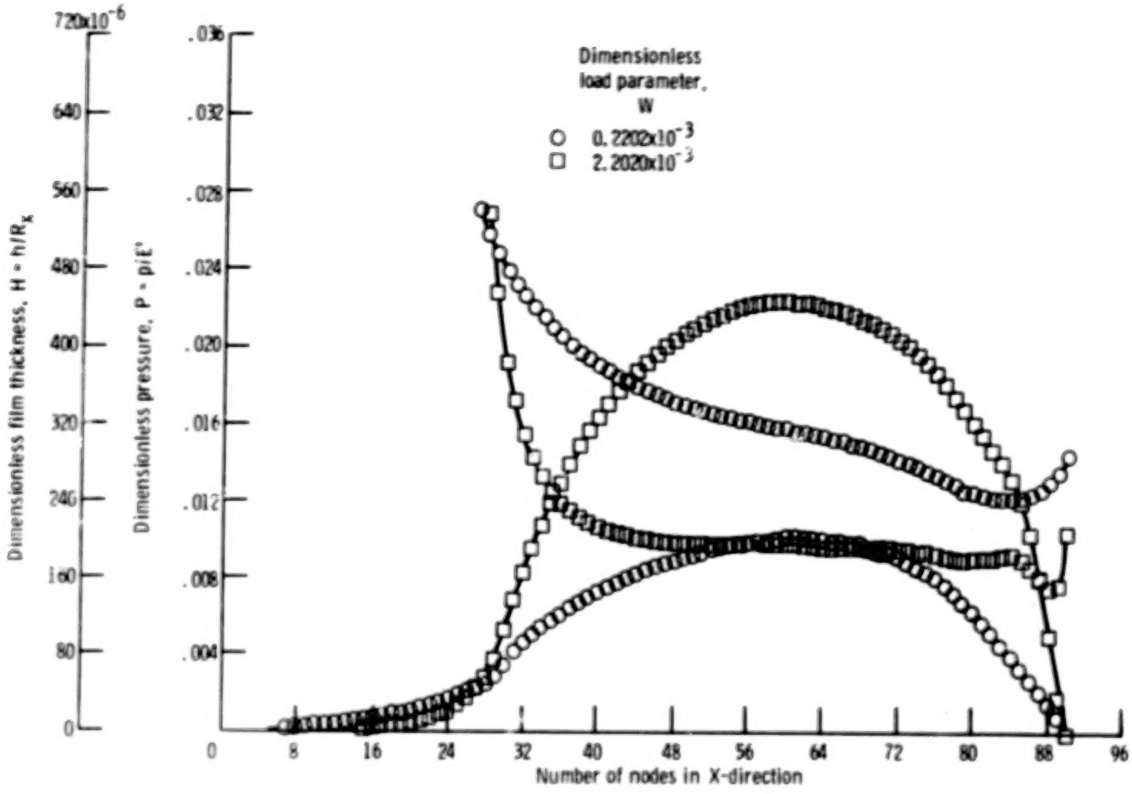

Figure 8. - Variation of dimensionless pressure and film thickness on X-axis for dimensionless load parameters W of 0.2202×10^{-3} and 2.202×10^{-3}. The value of Y is held fixed near axial center of contact.

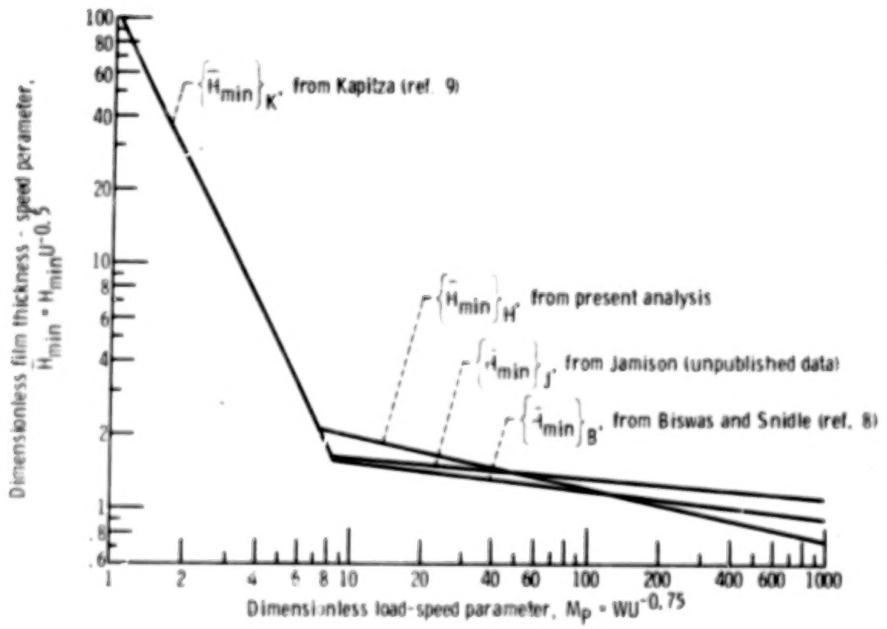

Figure 9. - Comparison of different investigators' results.

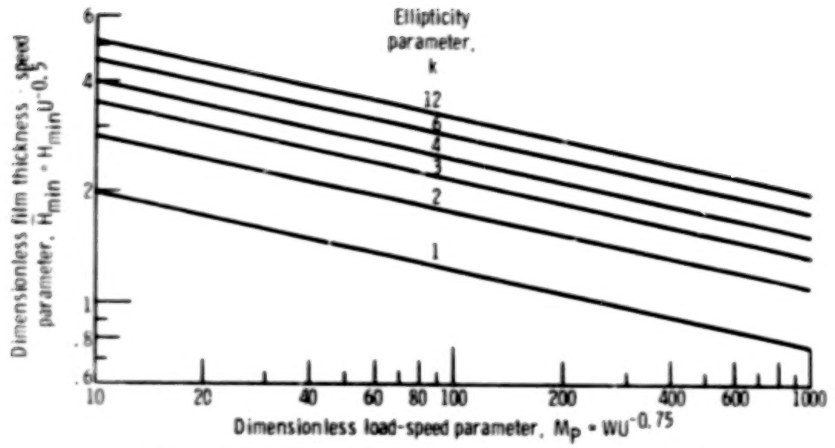

Figure 10. - Effect of dimensionless load-speed parameter on dimensionless minimum film thickness - speed parameter for six ellipticity parameter values.

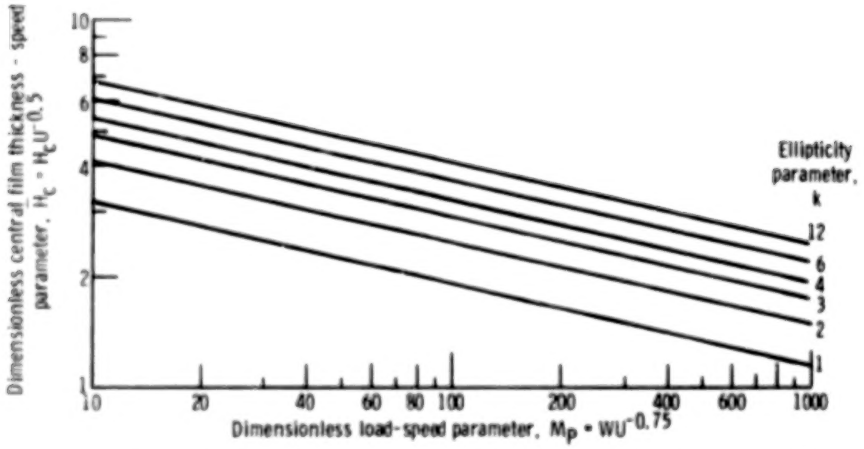

Figure 11. - Effect of dimensionless load-speed parameter on dimensionless central film thickness - speed parameter for six ellipticity parameter values.

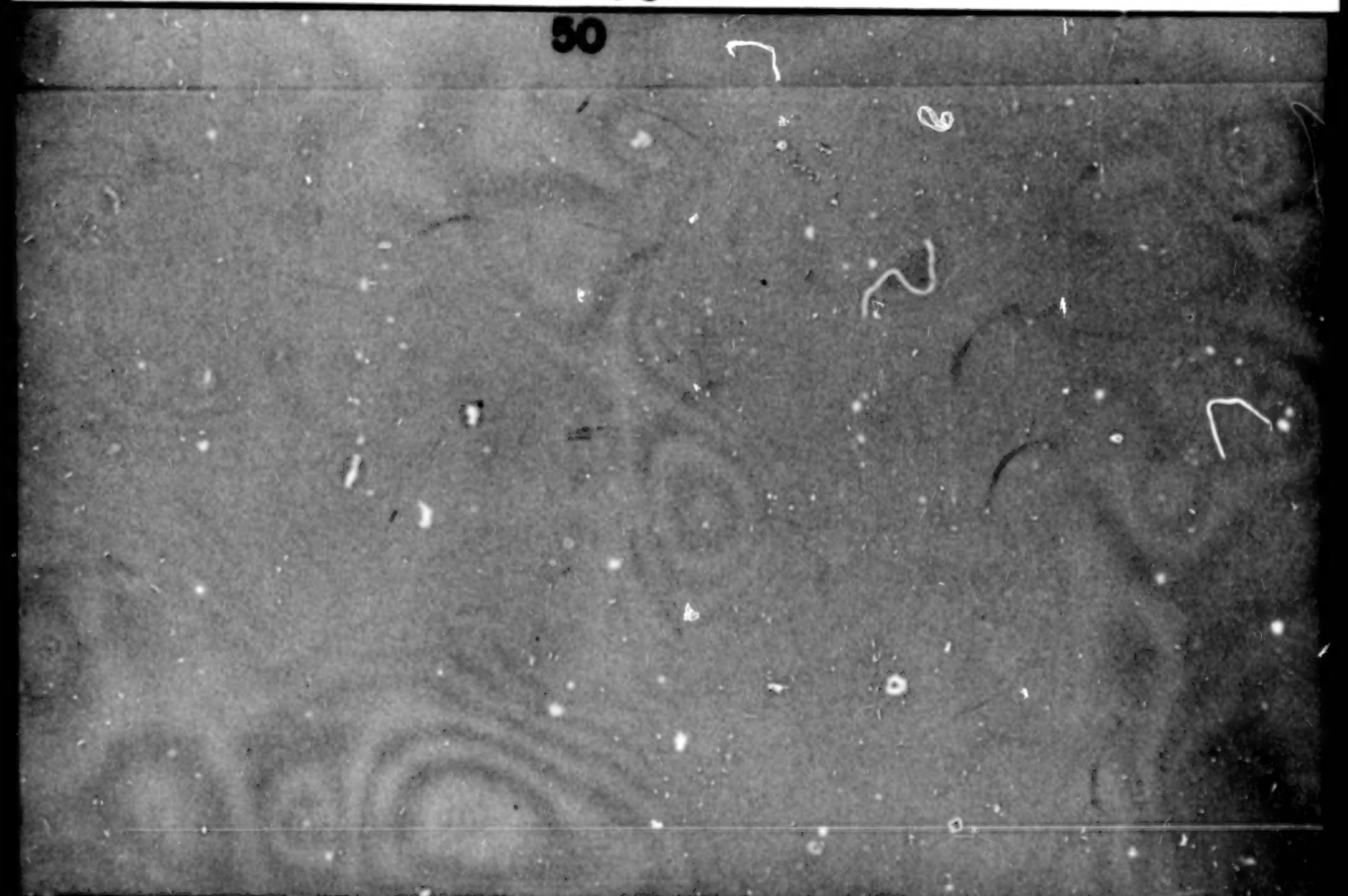
90
50

END

5.19 78